A new FRET biosensor enlightens cAMP signalling in budding yeast

Dennis Botman[1], Tom G. O'Toole[2], Joachim Goedhart[3], Frank J. Bruggeman[1], Johan H. van Heerden[1] & Bas Teusink[1*]

[1]Systems Biology Lab/AIMMS, Vrije Universiteit Amsterdam, De Boelelaan 1085, 1081 HV, Amsterdam, The Netherlands.
[2]Department of Molecular Cell Biology and Immunology, Vrije University Medical Center, De Boelelaan 1085, 1081 HV, Amsterdam, The Netherlands.
[3]Section of Molecular Cytology, van Leeuwenhoek Centre for Advanced Microscopy, Swammerdam Institute for Life Sciences, University of Amsterdam, Science Park 904, 1098 XH, Amsterdam, The Netherlands.
*Correspondence should be addressed to Bas Teusink (email: b.teusink@vu.nl)

Abstract

The cAMP-PKA signalling cascade in budding yeast regulates adaptation to changing environments. Many questions remain about the function of cAMP dynamics, largely because no robust method for *in vivo* cAMP measurements exists for yeast. Here we developed yEPAC, a FRET-based biosensor for cAMP measurements in yeast. We show that this biosensor can be used in flow cytometry, allowing for high-throughput single cell-level quantification that complements microscopy measurements. We quantified both steady-state cAMP levels and dynamic changes in response to sudden nutrient transitions. Steady-state cAMP levels were found to correlate with growth rate (rather than glycolytic flux) and were independent of extracellular sensing. During transitions, a cAMP-peak differentiates between different carbon source transitions, and is generated only when switching from non- or slowly-fermentable sugars to rapidly fermentable ones. Furthermore, generation of the cAMP peak is mediated by a combination of extracellular sensing and metabolism; deficits in either results in a largely diminished response. Moreover, the cAMP peak follows Weber's law; its height scales with the relative, and not the absolute, change in glucose. This means that cells respond to small changes in extracellular glucose when the initial level is low, but ignore these changes when this level is high. Lastly, we speculate that the cAMP peak height conveys information about prospective growth rates, especially for fermentable sugars. In conclusion, our yEPAC-sensor makes possible new avenues for understanding yeast physiology, signalling and metabolic adaptation.

Introduction

Saccharomyces cerevisiae, or budding yeast, is a unicellular organism that lives in continuously changing environments to which it has to adequately adapt to stay competitive. To do so, yeast cells sense changes in nutrient availability and generate signals that they use as cues to adapt their physiological behaviour such as cellular metabolism and growth. For yeast, the most preferred carbon source is glucose, and it has evolved various signalling pathways responsive to its concentration[1–3]. One of these pathways is the cAMP-PKA pathway. Activation of cAMP-PKA occurs when derepressed cells are transitioned to an environment containing an abundant fermentable carbon source. This results in a transient increase of cAMP on a short timescale (i.e. seconds-minutes) and subsequent relaxation to an elevated steady level[4,5]. Activation of the cAMP-PKA pathway occurs via two distinct routes. First, import and metabolism of fermentable sugars activates Ras, stimulated by intracellular acidification[4,6,15,7–14].

Ras, in turn, activates the adenylate cyclase Cyr1 to produce cAMP. Second, the G-protein coupled receptor Gpr1 senses extracellular glucose and activates Cyr1 via Gpa2 (a G_α protein)[4,6,23,9,16–22]. Increased cAMP levels lead to activation of PKA, by causing dissociation of the regulatory subunit Bcy1 from the PKA subunits[24–26]. Activated PKA inhibits the stress-related transcription factors Msn2, Msn4 and the Rim15 protein kinase[27–30]. Moreover, PKA induces trehalose and glycogen breakdown[31–33] and increases levels of the glycolytic activator fructose-2,6-bisphosphate[34–36]. Altogether, activation of the cAMP-PKA pathway induces a shift from a slow growth or stress-resistant physiological state to a fast growing fermentative one.

A rise in cAMP is transient, due to its rapid degradation by phosphodiesterase 1 and 2[37–39]. Moreover, the signalling cascade itself is inhibited via feedback inhibition through active PKA (which inhibits various cAMP signalling components). Additionally, cAMP signalling is inhibited by Ira1, Ira2 (which inhibits Ras) and by Rgs2 (which inhibits Gpa2) and these inhibitions also give rise the transient nature of the response[37,38,40–44]. In contrast to the dynamic response to nutrient transitions, steady-state levels of cAMP have been less well studied. A few studies suggest that the glycolytic intermediate fructose-1,6-bisphosphate is an activator of Ras and determines the basal cAMP levels[6,9,45].

Although much progress has been made on cAMP-PKA signalling in yeast, various questions still remain. For the most part, characterisations were performed using solely glucose (or fructose) as fermentable carbon source. Therefore, cAMP responses to many other carbon sources or to stress-conditions are still largely unexplored. Since only a few conditions are generally studied, input-output characterisations of cAMP-PKA signalling are scarce. In particular the determination of steady-state cAMP levels remains difficult using currently available methods, and for this reason many of the functional implications of basal cAMP levels are still under debate[4,46–48]. Finally, it is still unknown whether heterogeneity occurs in single-cell cAMP responses; Cell-to-cell heterogeneity is especially relevant for industrial bioprocessing where glucose-signalling heterogeneity can affect industrial efficiency[49–52].

To address these questions, we developed a genetically-encoded biosensor for cAMP. We adapted an EPAC-based FRET sensor originally developed for mammalian cells[53,54] for use in budding yeast. The resulting yeast-EPAC (yEPAC) sensor contains pH-robust fluorescent proteins (FPs), measures cAMP with high selectivity and shows a high FRET ratio change. This enables convenient intracellular measurements of cAMP in living single-yeast cells for the first time. Using both flow cytometry and microscopy, we characterised cAMP responses at the single-cell level under various steady-state growth conditions, and in response to various nutrient transitions. Furthermore, we used flow-cytometry to quantify cellular heterogeneity in cAMP-dynamics during carbon source transitions. Combined, these measurements revealed several novel insights, including a linear relation between cAMP levels and growth rates at steady-state, and a strong dependence of cAMP peak height on the added carbon source and pre-growth conditions. Against a fermentative background, the amplitude of the cAMP response (peak height) is a measure for the relative change in glucose concentration, but against a respiratory background, peak height upon sugar addition appears to predict the extent of fermentative growth.

Material and methods

Fluorescent protein plasmids construction

The FRET-pairs mCherry-T2A-mTurquoise2 (mTq2), tagRFP-T2A-mTq2, tagRFPT-T2A-mTq2 and tdTomato-T2A-mTq2 in pDRF1-GW were previously constructed[55]. mCherry-mTq2, tagRFP-mTq2 and tagRFPT-mTq2 in a clontech-style C1 mammalian expression vector were obtained from Mastop et al.[56], digested using NheI and NotI (New England Biolabs, Ipswich, Massachusetts, USA), and ligated with T4

ligase (New England Biolabs) in the yeast expression vector pDRF1-GW [55], digested with the same restriction enzymes.
mTq2 in pDRF1-GW was created by performing a PCR, using KOD polymerase (Merck-Millipore, Burlington, Massachusetts, USA) on mTq2-C1 using forward primer 5'-AGGTCTATATAAGCAGAGC-3' and reverse primer 5'-TAGCGGCCGCTTACTTGTACAGCTCGTCCATG-3'. Next, the product and pDRF1-GW were digested with NheI and NotI and the PCR product was ligated into pDRF1-GW using T4 ligase, generating mTq2 in pDRF1-GW.

yEPAC construction

mTq2Δ-Epac (CD,ΔDEP)-cp173Venus-cp173Venus (Epac-SH188) was a kind gift of dr. Kees Jalink. A PCR with KOD polymerase was performed on tdTomato-C1, using forward primer 5'-TAGAGCTCATGGTGAGCAAGGGCGAGG-3' and reverse primer 5'-GCGGCCGCTTACTTGTACAGCTCGTCCATGCCG-3'. Next, both the PCR product and Epac-SH188 were digested, using SacI and NotI (New England Biolabs). The PCR product was ligated into Epac-SH188 using T4 ligase, replacing cp173Venus-cp173Venus for tdTomato. The adapted sensor and pDRF1-GW were digested using NheI and NotI and the sensor was ligated into pDRF1-GW, generating yEPAC (mTurquoise2Δ-Epac(CD,ΔDEP)-tdTomato in pDRF1-GW).

Yeast transformation

Strains used in this study are described in table 1. These strains were transformed exactly as described by Gietz and Schiestl[57].

In vitro characterisation

W303-1A WT cells transformed with pDRF1-GW and yEPAC were grown overnight at 200 rpm and 30°C in 1x yeast nitrogen base (YNB) medium without amino acids (Sigma Aldrich, Stl. Louis, MO, USA), containing 100 mM glucose (Boom BV, Meppel, Netherlands), 20 mg/L adenine hemisulfate (Sigma-Aldrich), 20 mg/L L-tryptophan (Sigma-Aldrich), 20 mg/L L-histidine (Sigma Aldrich) and 60 mg/L L-leucine (SERVA Electrophoresis GmbH, Heidelberg, Germany). The next day, cells were diluted and grown to an OD_{600} of approximately 3 in 50 mL of the same medium. Next, cells were kept on ice and washed twice in ice-cold 20 mL 0.01 M KH_2PO_4/K_2HPO_4 buffer at pH7 containing 0.75 g/L EDTA (AppliChem GmbH, Darmstadt, Germany). After the last wash step, cells were resuspended in 2 mL of 0.01 M KH_2PO_4/K_2HPO_4 buffer containing 0.75 g/L EDTA. Cells were washed twice in 1 mL of ice-cold 0.1 M KH_2PO_4/K_2HPO_4 buffer at pH7.4 containing 0.4 g/L $MgCl_2$ (Sigma-Aldrich). Cells were transferred to screw cap tubes pre-filled with 0.75 grams of glass beads (425-600 µm) and lysed using a FastPrep-24 5G (MP Biomedicals, Santa Ana, CA, USA) with 8 bursts at 6 m/s and 10 seconds per burst. Afterwards, the lysates were centrifuged for 15 minutes at 21000 g and the cell-free extracts were snap-frozen in liquid nitrogen and stored at -80°C for later use.
Per sample, 5 wells of a black 96-well microtitre plate (Greiner Bio-One) were filled with 40 µL of cell-free extract. Fluorescence spectra were recorded after successive additions of cAMP (Sigma-Aldrich) using a CLARIOstar platereader (BMG labtech, Ortenberg, Germany). Spectra were recorded with 430/20 nm excitation and 460-660 nm emission (10 nm bandwidth). Fluorescence spectra were corrected for background fluorescence (by correcting for fluorescence of W303-1A WT expressing the empty pDRF1-GW plasmid) and FRET ratios were calculated by dividing donor over acceptor fluorescence. The data was fitted to the Hill equation (equation 1)[54], with cAMP denoting the cAMP concentration, K_d the dissociation constant, and n the Hill-coeffecient.

$$FRET\ ratio = \frac{cAMP^n}{K_d^n + cAMP^n} \qquad \text{(eq. 1)}$$

ConA solution

Concanavalin A (ConA) was prepared as described by Hansen et al., 2015[58]. In brief, 5 mg of ConA (Type IV, Sigma Aldrich) was dissolved in 5mL PBS at pH6.5, 40 mL H_2O, 2.5mL of 1 M $MnCl_2$ and 2.5 mL of 1 M $CaCl_2$ and stored at -80°C.

Microscopy

Strains used in this study are described in table 1. These strains (expressing yEPAC) were grown overnight at 200 rpm and 30°C in 1x YNB medium without amino acids, containing 20 mg/L adenine hemisulfate, 20 mg/L L-tryptophan, 20 mg/L L-histidine, 60 mg/L L-leucine and either 1% Ethanol (v/v, VWR International, Radnor, PA, United States of America), 1% glycerol (v/v, Sigma Aldrich), 100 mM pyruvate (Sigma Aldrich) or 111 mM galactose (Sigma Aldrich). Next, cells were diluted in the same medium and grown to an OD600 of maximally 1.5 and with minimal 5 cell divisions. The cultures were transferred to a 6-well microtitre plate containing cover slips pre-treated ConA to immobilize the cells. Afterwards, the coverslip was put in an Attofluor cell chamber (Thermofisher Scientific, Waltham, MA, USA) and 1 mL of fresh medium was added. Samples were imaged with a Nikon Ti-eclipse widefield fluorescence microscope (Nikon, Minato, Tokio, Japan) at 30°C equipped with a TuCam system (Andor, Belfast, Northern Ireland) containing 2 Andor Zyla 5.5 sCMOS Cameras (Andor) and a SOLA 6-LCR-SB power source (Lumencor, Beaverton, OR, USA). Fluorescent signals were obtained using a 438/24 nm excitation filter. The emission was separated by a 552 nm long-pass (LP) dichroic filter in a TuCam system. A 483/32 nm and 593/40 nm emission filter-pair was used for the detection of donor and acceptor emission, respectively (all filters from Semrock, Lake Forest, IL, USA). Perturbations were performed by adding 1x YNB medium containing the same amino acids as described before with 10x concentrated carbon source or KCl to the cell chamber to the desired concentration. Per condition, at least 2 biological replicates were obtained. Cells were segmented and fluorescence was measured with an in-house FiJi macro (NIH, Bethesda, MD, USA).

Table 1. *S. cerevisiae* strains used in this paper.

Strain	Genotype	Source
W303-1A WT	MATa, leu2-3/112, ura3-1, trp1-1, his3-11/15, ade2-1, can1-100	J. Thevelein, Katholieke Universiteit Leuven, Belgium
YSH757	W303-1A glk1Δ::LEU2 hxk1Δ::HIS hxk2Δ::LEU2	Stefan Hohmann (Chalmers University of Technology, Gotenburg, Sweden)
W303-1A gpr1Δ	W303-1A gpr1Δ::LEU2	Joris Winderickx, Katholieke Universiteit Leuven, Belgium.
W303-1A Cyr1^{K1876M}	W303-1A Cyr1^{K1876M}	Joris Winderickx, Katholieke Universiteit Leuven, Belgium.

Growth experiments

Cells expressing pDRF1-GW and yEPAC were grown to midlog as described for microscopy with medium containing 1% ethanol. Next, cells were washed and resuspended to an OD_{600} of 1 with the same medium with the carbon source omitted. Cells were transferred to an OD of 0.05 in a 48-well microtitre plate containing 480 µL of fresh medium with either 0.1% ethanol, 10 mM galactose or 10 mM glucose. The cells were grown in a Clariostar plate reader at 30°C and 700 rpm orbital shaking. OD_{600} was measured every 5 minutes.

Fluorescence lifetime imaging and spectral imaging

W303-1A WT cells expressing mCherry-mTq2, mCherry-T2A-mTq2, tagRFP-mTq2, tagRFP-T2A-mTq2, tagRFPT-mTq2, tagRFPT-T2A-mTq2, tdTomato-mTq2 and tdTomato-T2A-mTq2 were grown for at least

2 weeks on 2% agarose plates containing 6.8 g/L YNB without amino acids, 100 mM glucose, 20 mg/L adenine hemisulfate, 20 mg/L L-tryptophan, 20 mg/L L-histidine and 60 mg/L L-leucine. Frequency domain FLIM was performed as described before[56]. Briefly, 18 phase images were obtained with a RF-modulated image intensifier (Lambert Instruments II18MD, Groningen, The Netherlands) set at a frequency of 75.1 MHz coupled to a CCD camera (Photometrics HQ, Tucson, AZ, USA) as detector. mTq2 was excited using a directly modulated 442 nm laser diode (PicoQuant, Berlin, Germany). Emission was detected using a 480/40 nm filter. The lifetimes were calculated based on the phase shift of the emitted light (τϕ). Per sample, 3 replicates were recorded.
Emission spectra of a donor-acceptor fusion protein or unfused equimolar expressed donor and acceptor were acquired as described previously[56]. In brief, excitation was at 436/20 nm and the emission was passed through a 80/20 (transmission/reflection) dichroic mirror and a 460 nm LP filter. Individual spectra were corrected for expression level by quantifying the intensity of the acceptor by excitation at 546/10 nm and detection with a 590 nm LP filter. Per sample, 3 replicates were measured.

Flow cytometry

W303-1A strains expressing yEPAC, pDRF1-GW and mTq2 were grown as described for microscopy. Flow cytometry was performed using an BD INFLUX cell sorter (Becton Dickinson, Franklin Lakes, NJ, USA), with a 140 µm nozzle and a sheath pressure of 6 psi to run the samples. The sorter was equipped with a 200 mW Solid State 488 nm laser focused on pinhole 1, a 75 mW Solid State 561 nm laser focused on pinhole 3 with a laser delay of 18.17 µsec and a 100 mW Solid State 445 nm laser focused on pinhole 5 with a laser delay of 37.11 µsec. PMTs (photo multiplier tubes) for the 445 nm laser and the 488 nm laser were assimilated in trigon detector arrays that use serial light reflections – moving from the longest wavelengths to the shortest – to collect the dimmest emission signals first. The 445 nm trigon array was configured with a 610/20 nm bandpass filter in detector A and a 520/35 nm bandpass filter (preceded by a 502 nm LP filter) in detector B. The 488 trigon array was configured with a 692/40 nm bandpass (preceded by a 600LP) in detector A, a 530/40 nm bandpass (preceded by a 520 LP) in detector B and a 488/10 bandpass in detector C (SSC). PMTs for the 561 laser were assimilated in an octagon detector array. Acceptor emission was measured in detector D which was filtered with a 610/20 bandpass (preceded by a 600LP). Per condition, at least 2 biological replicates were obtained. To measure FRET ratios of YSH757 cells in glucose or sucrose containing medium, cells were grown to midlog in 1% ethanol as previously described. Next, 100 mM glucose or 111 mM sucrose was added to the medium and cells were incubated for at least 5 hours (1 replicate for this condition). All events were corrected for background fluorescence (median fluorescence of cells expressing pDRF1-GW), bleedtrough corrected and filtered for saturating or low fluorescence and scatter values. Next, per day, all FRET ratios were normalized to the median FRET ratio of W303-1A WT in 2% glucose.

Data analysis

All data were analysed and visualized using R version 3.5.1 (R Foundation for Statistical Computing, Vienna, Austria). For analysis, cell with low fluorescence (i.e. below 50 A.U. fluorescence counts) were filtered and per cell, FRET ratios were normalized to the mean FRET ratio before the perturbation (baseline). Dose-response kinetics were fitted using equation 2 with $Peak_{max}$ denoted as the maximal peak height that can be obtained, glucose the amount of glucose pulsed and $K_{0.5}$ the glucose amount that induces half the maximal peak height.

$$Peak\ height = \frac{Peak_{max} \cdot glucose}{K_{0.5} + glucose} \qquad \text{(eq. 2)}$$

Results

Engineering of a versatile EPAC sensor for cAMP quantifications in yeast

To measure cyclic AMP, we started with the EPAC sensor H188 from Klarenbeek et al., (2015), which contained mTq2Δ11 and tandem-cp173Venus as FRET pair[59]. In yeast, cAMP signalling is believed to be partly initiated by intracellular acidification, which occurs transiently when derepressed cells start to metabolize fermentable sugars[6,10]. Since Venus is pH sensitive[55,60], we opted to replace it for a pH-robust acceptor fluorescent protein (FP). We tested mCherry, tagRFP, tagRFP-T and tdTomato as potential acceptors, as we have previously shown that these proteins are more pH-insensitive[55]. We replaced the Venus acceptor for tdTomato as this was the best acceptor for mTurquoise2; It has a FRET efficiency of 23% and a substantial sensitized emission (Fig. S1, table S1), making it very suitable for ratiometric fluorescence readouts. This yielded yEPAC, an EPAC-H188 variant with mTq2Δ11 and tdTomato as FRET pair.

In vitro calibration of yEPAC showed loss-of-FRET upon cAMP addition, and therefore, FRET ratios are presented as CFP/RFP ratios in this paper. We determined that yEPAC has a K_D of 4 µM for cAMP, which is comparable to the original H188 sensor (Fig. 1A); this K_D is in the range of physiological cAMP levels in yeast[37,61–63]. We performed various control experiment to characterize the performance and potential of yEPAC. We confirmed that glucose addition to cells grown on a non-fermentable carbon source indeed gave a transient cAMP peak and that the Cyr1^{K1876M} mutation showed a diminished cAMP response (Fig. 1B), as described before[64]. As required, the non-responding sensor-variant yEPAC-R279L showed minimal FRET change upon a glucose transition (Fig. 1B). Furthermore, the yEPAC sensor did not aggregate in cells and did not affect growth (Figs. 1C, S2). We also tested the maximal temporal resolution we could obtain. The mTq2-tdTomato FRET pair is highly photostable[55], making the FRET sensor useful for both extended (over many hours) and high temporal resolution (rapid frame rate) time-lapse movies. Using yEPAC, we could record cAMP responses up to 15 minutes with a 3 second time interval, i.e. 300 time-points (Fig. 1D, movie S1), without adverse photobleaching effects.

Lastly, we wondered whether we could expand the use of biosensors with flow cytometry. We grew cells on 1% EtOH and 100 mM glucose and measured steady-state FRET levels using microscopy and flow cytometry (Fig. 1E). Data obtained from both methods showed highly comparable results, indicating that flow cytometry (named flow-FRET in this manuscript) can indeed be used with our FRET sensor. This opened new possibilities since FRET levels can be measured in a truly high-throughput manner. We went one step further and tested whether we could measure dynamic FRET responses using flow-FRET. This approach provides a useful complement to microscopy, as it allows for hundreds to thousands of single-cells to be sampled per second. However, it cannot measure FRET in the same cells over time. We tested this method with additions of 2 or 100 mM glucose to ethanol grown cells (Fig. 1F). We obtained FRET ratios of 300-700 cells per second to determine cAMP responses. The dynamics were comparable to the microscopy-obtained data (Fig. 1F and S3). Of note, we did not observe non-responders, also not by the addition of 2 mM glucose. This is in agreement with the steady-state distributions, which did not show subpopulations (Fig. 1E).

In summary, our developed yEPAC sensor can be used to reliably measure cAMP in single yeast cells without adverse effects. Also, we show that our sensor can be used with flow cytometry, in addition to the conventional microscopy readouts, expanding its utility.

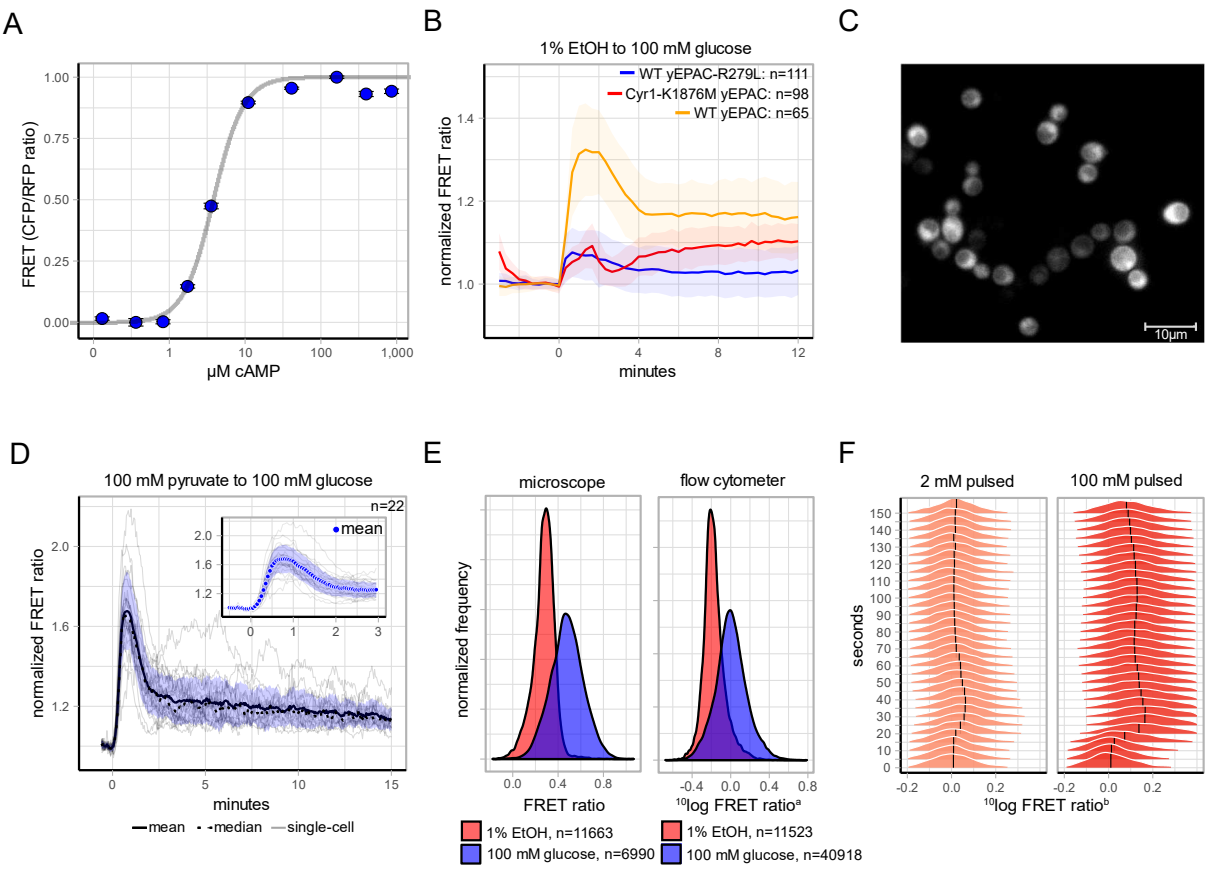

Figure 1. yEPAC characterisation. A) *In vitro* cAMP dose-response curve of yEPAC. Points indicate the mean FRET value of 5 replicates, error bars indicate SD. Solid line shows the Hill-fit (eq. 1). B) W303-1A WT cells expressing yEPAC or the non-responsive yEPAC-R279L and W303-1A cells that possessed the Cyr1^{K1876M} mutation were grown on 1% EtOH and pulsed with glucose at t=0 minutes. FRET signals were obtained and baseline normalized, lines show mean FRET ratios, shaded areas indicate SD. C) W303-1A cells expressing the yEPAC sensor show homogenous expression of the sensor. D) Pyruvate-grown W303-1A cells pulsed with 100 mM glucose at t=0 minutes. Inset shows the first 3 minutes after the pulse. FRET ratios are normalized to the baseline, solid lines show mean FRET ratios, dotted lines show median FRET ratios, grey lines show single-cell trajectories, shaded areas indicate SD. E) Normalized frequency distributions of yEPAC FRET ratios of cells grown on either 1% EtOH or 100 mM glucose by microscopy (left panel) or flow cytometry. F) Dynamic frequency distribution of FRET values after 2 and 100 mM glucose addition, respectively. W303-1A WT cells were pre-grown on 1% EtOH, a baseline was recorded (not shown in graph) and a glucose pulse was added at 0 seconds. Timepoints were binned for every 5 seconds. Percentages are v/v, abbreviations: EtOH, ethanol, [a]FRET ratio was normalized to cells grown on 100 mM glucose. [b]FRET ratios were baseline-normalized.

Flow-FRET reveal that steady-state cAMP levels correlate with growth rate

An open question we could explore with flow-FRET is whether steady-state cAMP levels differ among growth conditions and cAMP signalling mutants. The new flow-FRET method was used to determine single-cell steady-state cAMP levels in large populations (Fig. 2). The WT, receptor mutant (gpr1Δ) and Cyr1^{K1876M} strains all showed the same steady-state cAMP levels, when growing on glucose. In contrast, a triple hexokinase mutant (hxk1Δ, hxk2Δ, glk1Δ) that is unable to phosphorylate and metabolize glucose showed much lower cAMP levels, even after 5 hours of incubation in glucose. (Fig 2A). This suggested that it is not the available (and sensed) substrate concentration that determines basal cAMP levels, but possibly metabolic flux or growth rate.

To test this, we grew the W303-1A strains in various carbon sources to obtain growth rates ranging from 0.03 to 0.36 (Figs. 2B and S4, table 2). Steady-state levels of cAMP indeed scaled with growth rate (Spearman correlation, $r=0.96$, $p<0.01$), also when signalling mutants were included ($r=0.92$, $p<0.01$). Of note, the triple hexokinase strain, which did not show increased levels when incubated with glucose, did show increased cAMP levels when grown on galactose compared to ethanol (Fig. 2A, C). We conclude that steady-state cAMP levels correlate with growth rate.

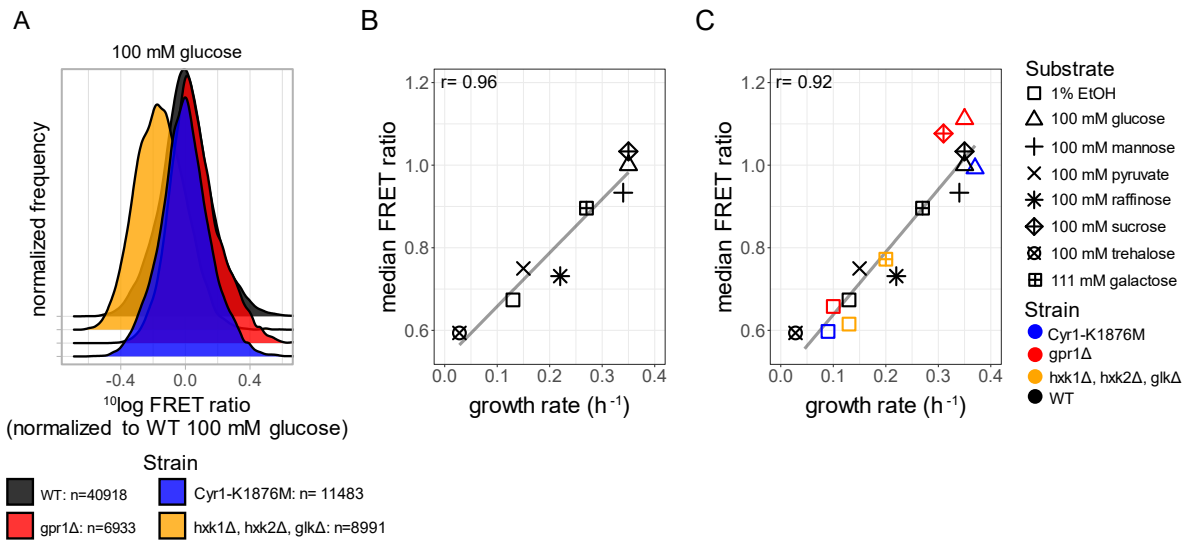

Figure 2. Flow-cytometry FRET data of W303-1A cells expressing yEPAC. A) Normalized frequency distributions of W303-1A mutants grown on glucose. FRET ratios were normalized to WT cells growing on 100 mM glucose. B) Flow cytometry data of W303-1A WT cells show a relation between growth rate and cAMP levels. C) Flow cytometry data of various W303-1A strains show that the relation between growth rate and cAMP levels is independent of the various inputs of cAMP signalling. For each biological replicate the median FRET value was calculated and normalized to the median of WT cells rowing on 100 mM glucose on the same day. Next, mean FRET ratio were calculated based on the median FRET ratio of all replicates. These values are depicted by the symbols in the graphs. The spearman correlation coefficient (r) is shown.

Table 2. FRET ratios of all strains grown on various carbon sources. For each biological replicate, the median FRET value was calculated, and normalized by division with the median value of WT growing on 100 mM glucose on the same day. Shown is the mean value for all biological replicates. *These strains were incubated for 5 hours in medium with glucose or sucrose.

W303-1A strain	Substrate	Mean FRET ratio	Growth rate (h^{-1})
WT	1% EtOH	0.67	0.13
WT	100 mM glucose	1	0.35
WT	100 mM pyruvate	0.75	0.15
WT	100 mM sucrose	1.03	0.35
WT	111 mM galactose	0.90	0.27
WT	100 mM raffinose	0.73	0.22
WT	100 mM mannose	0.93	0.34
WT	100 mM trehalose	0.59	0.03
hxk1Δ, hxk2Δ, glk1Δ	1% EtOH	0.56	0.13
hxk1Δ, hxk2Δ, glk1Δ	100 mM glucose*	0.68	0
hxk1Δ, hxk2Δ, glk1Δ	100 mM sucrose*	0.68	0
hxk1Δ, hxk2Δ, glk1Δ	111 mM galactose	0.77	0.20
gpr1Δ	1% EtOH	0.66	0.10
gpr1Δ	100 mM glucose	1.11	0.35
gpr1Δ	100 mM sucrose	1.07	0.31
$Cyr1^{K1876M}$	1% EtOH	0.60	0.09
$Cyr1^{K1876M}$	100 mM glucose	0.99	0.37

cAMP peak heights follow the Weber-Fechner law

Until now, we measured cAMP responses for transitions to saturating glucose amounts (Figs. 1B, D). However, we wondered how cAMP levels would change in response to lower amounts of glucose. We pulsed W303-1A cells grown on ethanol with glucose ranging from 0 to 50 mM of glucose. Normalized peak heights of these transitions showed a saturating dose-response with a $K_{0.5}$ of 3.1 mM and a maximal peak height of 1.38 normalized FRET values (Fig. 3A).

The dose-response data were generated against a background of zero glucose, and indicated that yeast cells are able to detect small amounts of glucose. However, we hypothesized that any advantage cells may reap from responding to a change in sugar availability, will depend largely on the amount of sugar already in the environment (i.e. the background level). This means that a cell should respond to small glucose changes when glucose levels are low, but should be less sensitive to the same (absolute) changes when glucose levels are already high. We therefore tested whether the magnitude of the glucose-induced cAMP peak heights scale with the relative change of the glucose concentration instead

of the absolute change, *i.e.* whether it obeys the Weber-Fechner law[65]. We incubated cells in media with various background concentrations of glucose and subsequently added various amounts of glucose (Figs. 3B, D, E, F). Indeed, we found comparable responses between transitions with the same relative change but with different absolute amounts of glucose pulsed (Fig. 3B). Because systems that detect relative changes add up inputs with positive and negative responses[66], we also tested the application of two such inputs simultaneously. First, we identified salt stress as a negative input as this reduced cAMP levels transiently (Fig. S5). Indeed, addition of salt stress to cells reduces glucose-induced peak heights (Fig. 3C), which indicates that the cAMP peak height can measure relative glucose changes. Normalized peak heights decreased with increasing amounts of pre-incubated glucose, which shows that cells indeed change cAMP peak heights based on their background level (i.e. the pre-incubated glucose level). Moreover, the normalized peak heights relate better with the fold-change in glucose than with the absolute glucose change (Figs. 3E and 3F).

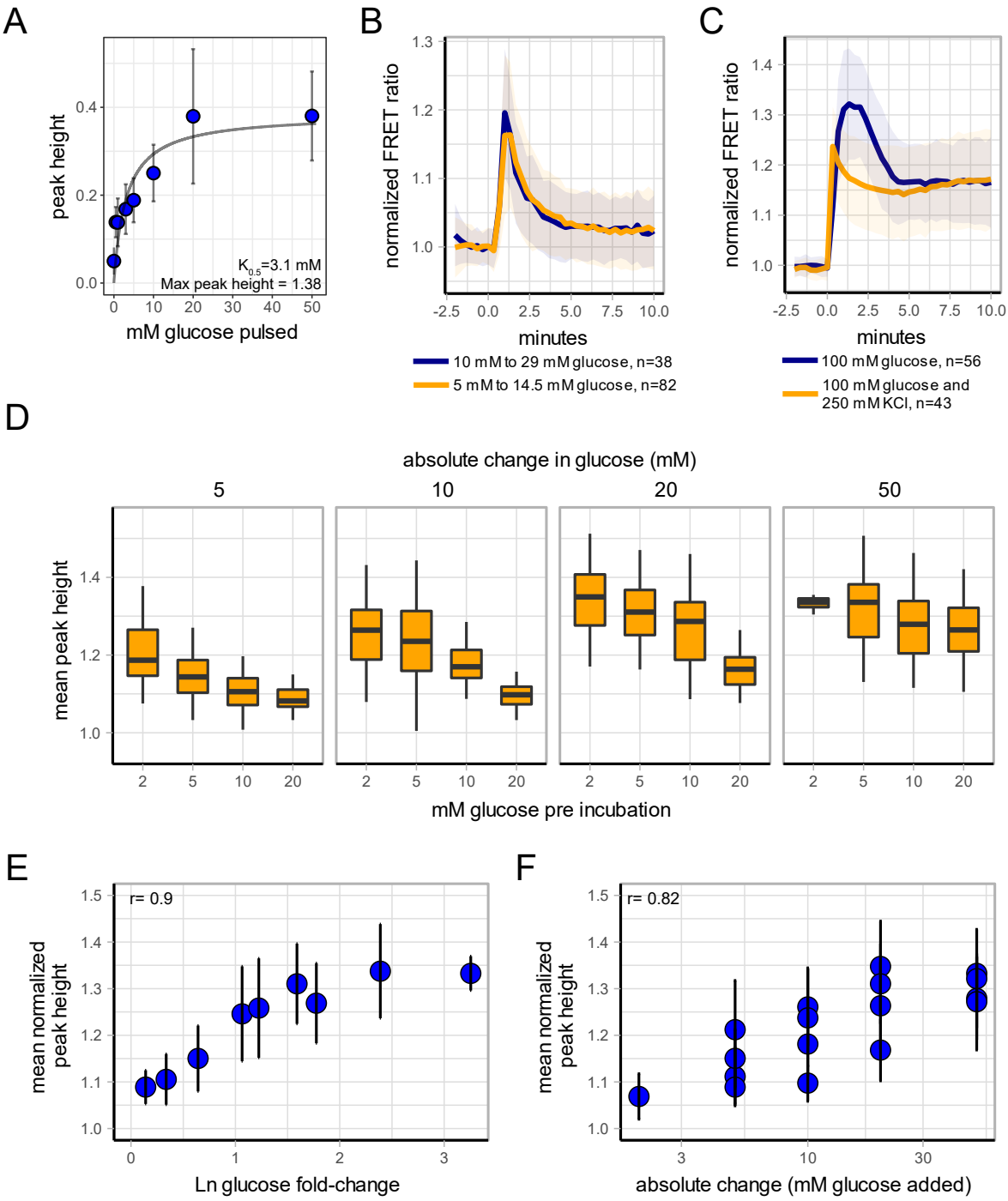

Figure 3. Dose-response and Weber-Fechner law experiments of cAMP. A) W303-1A cells expressing yEPAC were grown on 1% ethanol and various glucose concentrations were pulsed. Fitting peak heights versus the glucose concentration shows saturation kinetics with a $K_{0.5}$ of 3.1 mM. Dots indicate mean value, error bars indicate SD, grey line shows the fit using eq. 2. B) W303-1A cells expressing yEPAC were pre-incubated at either 5 or 10 mM glucose and a 2.9-fold change of glucose was performed. Lines show mean response, shaded areas indicate SD. C) W303-1A cells expressing yEPAC were grown on 1% EtOH and either 100 mM glucose or 100 mM glucose with 250 mM KCl was added. Lines show mean responses, shaded areas indicate SD. D) Population response of cAMP of cells expressing yEPAC. Cells were incubated at various initial amounts of glucose (depicted below each graph) and various amounts of glucose were added (depicted above each graph). Dots show mean populations response, error bars indicate SD. E) Peak heights plotted against the log fold-change of various glucose transitions, dots indicate mean value, error bars indicate SD. F) Peak heights plotted against the absolute glucose added for transitions, dots indicate mean value, error bars indicate SD.

Next, we tested whether a fixed glucose fold-change pulse applied successively to the same population, elicits a similar peak response (Fig. 4). Indeed, we found that also in this case, the baseline-normalized peak height scales with the relative glucose change and not the absolute amount. (Fig. 4A, B). For individual cells we found only a weak correlation between normalized-peak heights of the first versus the second perturbation.(Fig. 4C). This indicates that at the single cell level, the relative change is rather noisy, where the population response is robust. However, an increased time between the fold-changes may improve Weber-Fechner law detection at single-cell level. In line with this, we found that perturbations within a shorter timescale (i.e. every 10 minutes) show deteriorated Weber-Fechner law responses (Fig. S6). In these transitions, cells largely lose their ability to detect relative glucose changes. This suggests that the minimal time scales at which cells can adapt their glucose threshold is in the order of 20-30 minutes, and therefore the mechanism likely involves changes in protein expression.
In conclusion, we show that cAMP responses are sensitive to glucose changes when cells reside in low glucose environments. In high glucose environment cAMP responses are rescaled, making the cAMP response relative to the current glucose levels cells are in.

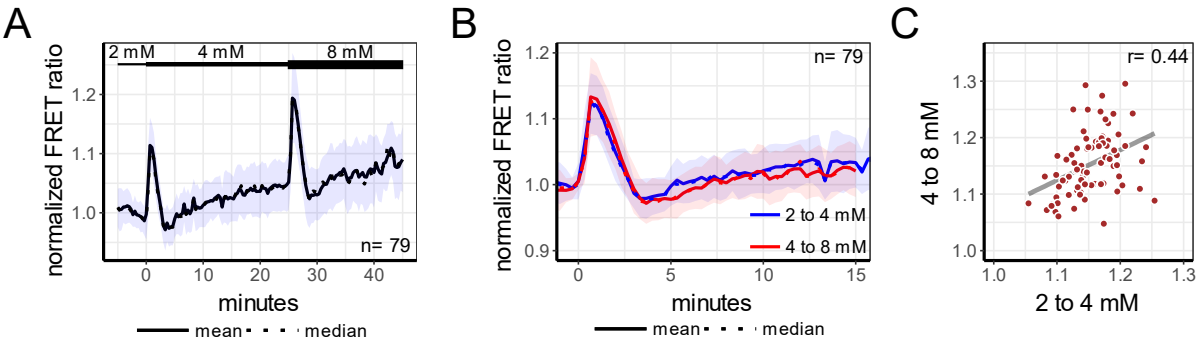

Figure 4. Weber-Fechner law of the same cells in time. A) W303-1A cells expressing yEPAC were pre-incubated on 2 mM glucose. Afterwards, cells were transitioned to 4 mM glucose at t=0 minutes and transitioned again to 8 mM at t=25 minutes, resulting in a two-fold change each time. Solid line shows the population mean response, dotted line shows median response, normalized to the first 5 minutes. B) Responses of the transitions performed in graph A, normalized to the last 3 frames before each transition. Solid line shows the population mean response, dotted line shows median response. Colour indicates the transition. C) Relation of normalized peak heights of single-cells between the first and second transitions. Shaded areas indicate SD. Dots represents single-cells, r-value shows the Spearman correlation coefficient ($p < 0.01$).

cAMP responses are carbon-source transition dependent

The cAMP signalling cascade is well known and characterised for its transitions from non-fermentable carbon sources to glucose. However, less data is available for other transitions. Therefore, we quantified the cAMP response for transitions between a variety of carbon sources. W303-1A WT cells were grown in medium containing 1% ethanol (v/v), 1% glycerol (v/v), 100 mM pyruvate or 111 mM galactose and subsequently pulsed with saturating amounts of either glucose, fructose, galactose, mannose or various oligosaccharides. This resulted in 18 different transitions for which the cAMP levels were monitored (Fig. 5).
Among the added sugars, only sucrose, glucose and fructose induced clear cAMP peaks. Addition of sucrose gave the highest peak and fructose the lowest. Cells pulsed with galactose or mannose did not show a cAMP peak. Mannose is known as an antagonist of Gpr1[21,22] and galactose is not a Gpr1 activator, which suggests that Gpr1 regulates the height of the cAMP peak. Noteworthy is the observation that mannose-pulsed cells did show increased cAMP levels after 15 minutes, even though an initial peak-response was absent. cAMP dynamics also depended on the pre-growth condition, with glycerol and pyruvate grown cells producing significantly higher cAMP peaks compared to EtOH and galactose grown cells (Wilcoxon test, $p<0.01$). In line with the dynamic flow-FRET results, we did not observe subpopulations or non-responders in most transitions (Figs. S7 and S8). Occasionally, we found for sugars other than glucose that some cells exhibited deviated cAMP dynamics compared to the population response. These cells show no cAMP peak or steadily increasing cAMP levels throughout the time-lapse recording. Therefore, cAMP signalling appears very robust for glucose transitions, but shows less robustness for other sugars.

Transitions from one primary carbon source to another can alter the maximal obtainable growth rate of cells. We wondered if cAMP peak heights could contain information about this new potential growth rate. Figure 3C indeed suggests such a relation: all data appear to lie on a curve. This curve fits very well with a glucose-dependent curve obtained when the dose response kinetics of figure 3A (max peak height 1.38 and $K_{0.5}$ = 3.1 mM) is plotted against the growth rate inferred from published Monod kinetics with a maximal growth rate of 0.37 h^{-1} and a K_s of 0.1 mM[67]. Note that the cAMP peak height shows a sharp increase when a growth rate higher than 0.3 h^{-1} can be obtained, which is around the onset of overflow metabolism[68].

In summary, our results show that the cAMP dynamics are context dependent, and that -at least for transitions from EtOH to sugars tested here- the peak height corresponds to the growth rate that can be achieved in the new environment.

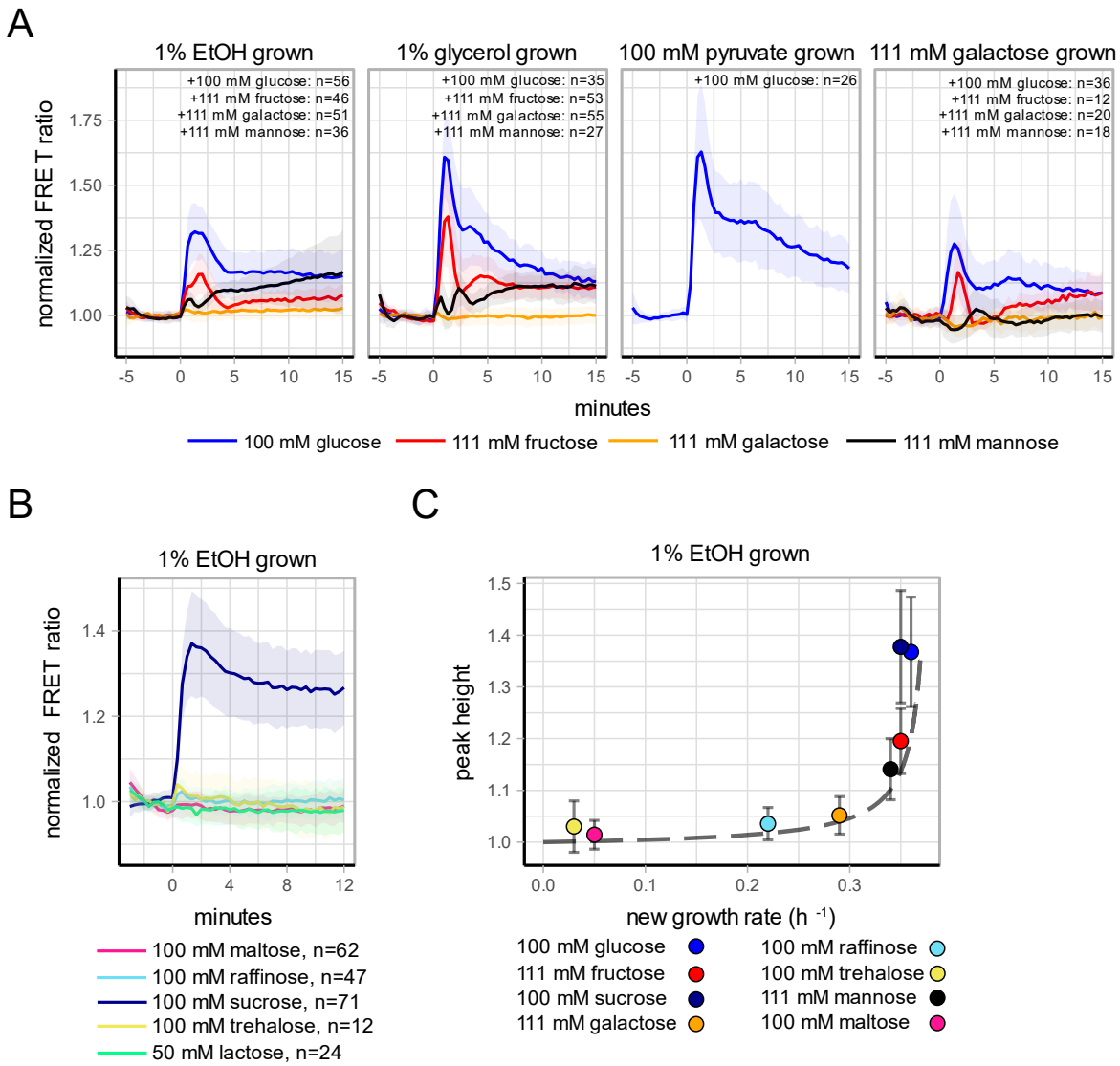

Figure 5. yEPAC FRET responses of various carbon transitions. A) Cells growing on various non-fermentative carbon sources (depicted above each graph) were pulsed with various sugars, depicted by line colour, at 0 minutes. Lines show mean FRET ratios, normalized to the baseline, shaded areas indicate SD. B) Cells growing on 1% ethanol were pulsed with various di- or trisaccharides and the FRET responses were recorded. Lines show mean FRET ratios, normalized to the baseline, shaded areas indicate SD, sugar was added at t=0 minutes. C) Peak heights of the transitions shown in A and B plotted against the maximal growth rate that can be obtained with the added carbon sources. Points show population mean, errorbars indicate SD, dotted line shows a glucose-dependent curve (obtained by plotting the dose response kinetics against Monod kinetics).

cAMP dynamics are affected by both Gpr1 signalling and sugar metabolism

Lastly, we examined which components of the signalling cascade affect the cAMP peak during transitions. cAMP signalling mutants were grown on medium containing 1% EtOH and pulsed with 2% glucose (Fig. 6). Deletion of either Gpr1, all three glucose phosphorylating enzymes (hxk1Δ, hxk2Δ, glk1Δ triple mutant) or the mutation in Cyr1 ($Cyr1^{K1876M}$) affected the transient peak in cAMP. Noteworthy, the hxk1Δ, hxk2Δ, glk1Δ mutant still showed a clear cAMP peak (although decreased compared to WT). This mutant does not display transient intracellular acidification upon glucose addition (since glucose cannot be metabolized), indicating that cAMP peak generation does not solely rely on acidification, or metabolism for that matter. Deletion of another input via the membrane bound Gpr1-sensor, had a similar effect on the cAMP peak response. In contrast to the triple kinase, the gpr1Δ mutant showed a slow increase in cAMP levels after glucose addition, which is in line with steady state measurements (Fig. 2) Since these two branches are known to regulate cAMP responses, we hypothesise that the residual cAMP response for both mutants are caused by the other cAMP signalling branch that is still functioning.

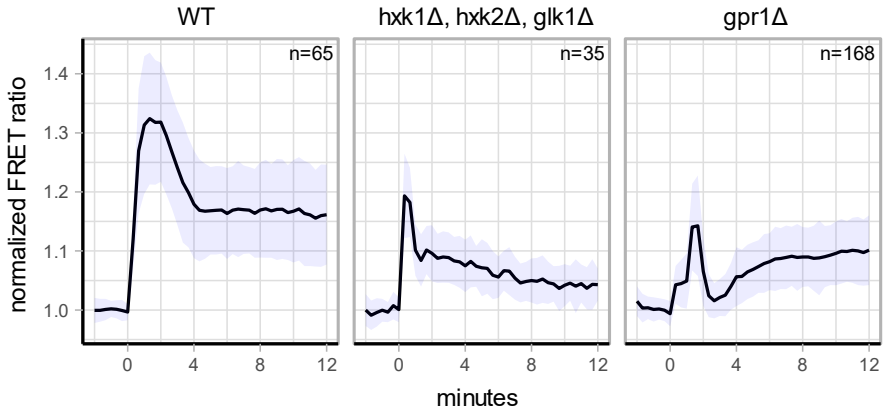

Figure 6. yEPAC FRET responses of various signalling mutants. The various cAMP signalling mutants in the W303-1A background were pulsed with 100 mM glucose at 0 minutes. Lines show mean FRET ratios, normalized to the baseline, shaded areas indicate SD.

Discussion

We present a FRET-based biosensor for dynamic, single-cell cAMP detection in yeast. Although a different FRET-based cAMP EPAC biosensor for budding yeast was published recently[69,70], we believe that our yEPAC has significant improvements. It shows an exceptionally high a FRET range, up to a normalized ratio change of 1.8. Moreover the usage of mTq2-tdTomato as a FRET pair results in decreased pH-sensitivity and increased photostability of the sensor, compared to YFP-CFP based sensors[55]. Signalling mutants and the non-responsive yEPAC variant showed good cAMP selectivity of the sensor. In line with this, we were able to expand the use of a FRET biosensor to flow cytometry. Through the high temporal resolution afforded by dynamic flow-FRET data, we found a clear secondary peak (Fig. S3) at high glucose concentrations. This peak was also present (Fig 5A), but not consistently observed, in the microscopy dataset. This oscillatory behaviour is in line with predictions from modelling efforts, but was not further explored in this study[71].

To our knowledge the combination of FRET biosensors with flow cytometry has not been used successfully before to study nutrient signalling. Here we used this powerful tool to obtain for the first time steady-state cAMP levels in yeast cells. These levels were found to correlate linearly with growth rate. This relation is independent of Gpr1, the presence of sugar kinases, or the $Cyr1^{K1876M}$ mutation. Recently, it was suggested that the glycolytic intermediate fructose-1,6-bisphosphate (F1,6bP) links glycolytic flux to Ras activation, thereby affecting cAMP production[45]. However, we show that ethanol-grown cells show higher cAMP levels compared to trehalose-grown cells. Ethanol-grown cells have a negative (gluconeogenetic) flux but a higher growth rate than cells growing on the glycolytic substrate trehalose, which indicates that basal cAMP levels relate with growth rate rather than glycolytic flux. A

relation between steady-state cAMP levels and growth rate makes a lot of sense when considering the overall downstream effects of PKA activity, *i.e.* activation of growth-supporting genes and suppression of stress-related genes.

Flow-FRET did not show clear non-responders or subpopulations in either steady-state populations or transitions during glucose transitions down to 2 mM. This was also confirmed with microscopy where no clear non-responders were found for glucose transitions (Fig. S7 and S8). However, we observed some heterogeneity in transitions with sugars that do not activate Gpr1[22]. Therefore, we hypothesise that this heterogeneity occurs from variation in the metabolism of the sugar, as observed before with carbon-source transitions[72,73]. These results show that the cAMP signalling cascade is robust, in contrast to what was found for pH[72] and recently for intracellular ATP dynamics as well (Botman et al, in preparation[73]). Apparently, as shown earlier[74], signalling glucose or metabolising it are different challenges to yeast cells.

In nature, yeast cells likely encounter large fluctuations in glucose availability, ranging from complete absence to saturating amounts of glucose. Until now, it was largely unknown how cAMP signalling reacts to a glucose increase when glucose is already present in the environment. Here we tested these glucose-to-increasing-amounts-of-glucose transitions. We found that cAMP peak heights seem to measure glucose changes relative to the background level of glucose, a property known as the Weber-Fechner law. Our analyses to test for Weber-Fechner law assume that each cell performs baseline-normalization. This could give an extra benefit by reducing variability among cells[66,75–77]. However, cells need time to establish a baseline between successive glucose-additions, since shortening the period between glucose additions no longer gave scaling of the cAMP peak height with the relative fold change (Fig. S6).

In order to reliably test for Weber's law, cAMP levels should be below saturation values of the yEPAC sensor. We validated this by comparing the normalized peak heights in response to saturating glucose amount (i.e. 50 mM glucose), when cells are pre-incubated at 2, 5, 10 and 20 mM glucose (Fig. 3D). Normalized peak heights were comparable, indicating that cAMP levels did not yet saturated the sensor. Our data therefore indicates that the cAMP pathway in yeast cells can detect (and adapt to) small glucose additions when glucose levels were low, but does not signal this change when glucose levels are high already. When cells are already fully fermentative, growing on glucose, the peak cannot indicate an increase in growth rate, but rather may signal how much sugar is present and whether or not cells should keep investing in fermentation and ribosomal biosynthesis

This is different when we added different carbon sources to fully respiratory, EtOH pre-grown cells. At this background, a consistent relation between peak height and the prospective growth rate on the pulsed sugar was found, for different sugars, and fitted the predicted growth rate for different glucose concentrations, based on Monod growth kinetics. This suggests that the peak height informs about growth. The cAMP signalling cascade is generally considered to mediate a switch cells to a fermentative (i.e. high growth rate) mode. This was consistent with our data, where cAMP peak height increased sharply around the onset of fermentation , *i.e.* under conditions that generate a growth rate higher than 0.3 h^{-1}, Fig. 5C). However, our results also show that cells without a clear cAMP peak (e.g. mannose pulsed cells) still obtain a high growth rate, without displaying a transient cAMP peak. Also the industrially important CEN.PK strain that has the K1876M mutation in Cyr1[64] does not show a peak but does ferment. So although we find clear and interesting relationships, their functional implications remain to be fully elucidated.

The cAMP responses to various other sugar transitions and in signalling mutants also showed that cAMP dynamics are complex and highly context dependent. Despite its complexity, we could infer several additional features about cAMP-signalling from these data.

First, nine sugars were tested and only sucrose (giving the highest peak) and its breakdown products, glucose and fructose induced a cAMP peak. It is remarkable that yeast developed a signalling cascade for only these sugars. On the other hand, sucrose is often the end-product of plant photosynthesis and therefore one of the most abundant sugars in plants[78]. In nature, yeast resides on plants or fruit and sensing extracellular sucrose conceivably improves yeast fitness, for example through stimulation of pseudohyphal growth[79].

Second, the data indicate that a cAMP peak is generated when either the initial metabolism of a sugar is sufficiently rapid or Gpr1 is activated. Combined activation is needed to achieve a maximal peak response. In response to glucose additions, both the gpr1Δ and the hxk1Δ, hxk2Δ, glk1Δ mutants show a transient cAMP-peak (Fig. 6), albeit significantly reduced. We found that fructose does not interact with Gpr1, but does induce a cAMP peak. In the case of fructose the peak is lower than peaks induced by the Gpr1 agonists sucrose or glucose, pointing to the amplifying effect of combined activation.
In stark contrast to the peak responses triggered by sucrose, glucose and fructose, mannose, which is an antagonist of Gpr1, does not show any cAMP peak. One explanation for the absence of a peak is signal-dampening through Gpr1 inhibition. Another explanation is that mannose gets transported much more slowly, since the hexose transporters have a lower V_{max} and higher K_m for mannose compared to glucose and fructose, which likely reduces the initial uptake rate of mannose[80,81]. Still, we found that mannose does trigger a gradual increase in cAMP levels shortly after its addition which is in line with the high growth rates that yeast can achieve on mannose. Accordingly, addition of galactose, which does not interact with Gpr1 and is not considered a rapidly-fermentable carbon source, does not induce a cAMP peak and does not yet show signs of a gradual increase in cAMP levels shortly after its addition. Indeed, cells growing on ethanol or glycerol are not immediately ready to metabolize galactose[82], and we expect the cAMP levels to gradually rise with the induction of galactose metabolism. A differential response to mannose by galactose- or ethanol-grown cells further underscores the effect of pre-growth conditions on the ability of cells to sense and respond to sudden sugar transitions. Mannose did not show the gradual increase in cAMP levels in galactose-grown cells as it did in ethanol grown cells. Galactose growth suppresses the expression of various high-affinity hexose transporters, such as HXT6 and 7, compared to growth on ethanol or glycerol[83–85]. Again, the affinity of HXT transporters for mannose is much lower than for glucose[80], and mannose uptake rate is therefore expected to be much lower in galactose grown cells than ethanol or glycerol grown cells, which may explain these observations.
Finally, we confirm that the cAMP peaks clearly originate partly from both the metabolism of the sugar as well as the Gpr1 receptor, as described before[17,21,86]. The hxk1Δ, hxk2Δ, glk1Δ and the gpr1Δ mutants both show diminished cAMP responses upon glucose addition. In line with previous studies, our data indicates that intracellular acidification is not a requisite as the hxk1Δ, hxk2Δ, glk1Δ shows no intracellular acidification (due to the absence of sugar phosphorylation) and still shows cAMP production[6,14,86].
Overall, our data combined shows that steady-state cAMP levels scale with the growth rate. The normalized peak height seems to be a signal for future growth rate on the pulsed sugar and is only produced when cells should switch to fermentative growth. Possibly, the peak height functions as a switch for rewiring to fermentable metabolism.

Acknowledgements

We thank Kees Jalink (Division of Cell Biology, The Netherlands Cancer Institute) for sharing mTurquoise2Δ-Epac(CD,ΔDEP)-cp173Venus-cp173Venus (Epac-SH188). We thank Juan Garcia Vallejo (Molecular Cell Biology & Immunology, VUmc) for his help with flow cytometry. We are grateful to Joris Winderickx (Functional Biology, KU Leuven) and Marco Siderius (Amsterdam Institute for Molecules, Medicines and Systems (AIMMS), Division of Medicinal Chemistry) for sharing W303-1A mutant strains. We thank Daan de Groot and Philipp Savakis for fruitful discussions.

Material requests

Requests for the yEPAC sensor should be addressed to Kees Jalink (Division of Cell Biology, Netherlands Cancer Institute, Plesmanlaan 121, 1066CX Amsterdam, the Netherlands, email k.jalink@nki.nl). Other material requests should be addressed to Bas Teusink (email: b.teusink@vu.nl)

References

1. Santangelo, G. M. Glucose Signaling in Saccharomyces cerevisiae Glucose Signaling in Saccharomyces cerevisiae. *Microbiol. Mol. Biol. Rev.* **70**, 253–282 (2006).
2. Rolland, F., Winderickx, J. & Thevelein, J. M. Glucose-sensing and -signalling mechanisms in yeast. *FEMS Yeast Res.* **2**, 183–201 (2002).
3. Rødkaer, S. V. & Faergeman, N. J. Glucose- and nitrogen sensing and regulatory mechanisms in Saccharomyces cerevisiae. *FEMS Yeast Res.* **14**, 683–696 (2014).
4. Beullens, M. *et al.* Studies on the mechanism of the glucose-induced cAMP signal in glycolysis and glucose repression mutants of the yeast Saccharomyces cerevisiae. *Eur. J. Biochem.* **172**, 227–31 (1988).
5. Eraso, P. & Gancedo, J. M. Use of glucose analogues to study the mechanism of glucose-mediated cAMP increase in yeast. *FEBS Lett.* **191**, 51–54 (1985).
6. Colombo, S. *et al.* Involvement of distinct G-proteins, Gpa2 and Ras, in glucose- and intracellular acidification-induced cAMP signalling in the yeast Saccharomyces cerevisiae. *EMBO J.* **17**, 3326–41 (1998).
7. Pardo, L. A., Lazo, P. S. & Ramos, S. Activation of adenylate cyclase in cdc25 mutants of Saccharomyces cerevisiae. *FEBS Lett.* **319**, 237–243 (1993).
8. Engelberg, D., Simchen, G. & Levitzki, A. In vitro reconstitution of cdc25 regulated S. cerevisiae adenylyl cyclase and its kinetic properties. *EMBO J.* **9**, 641–51 (1990).
9. van Aelst, L., Jans, W. H. & Thevelein, M. Involvement of the CDC25 gene product in the signal transmission pathway of the glucose-induced RAS-mediated cAMP signal in the yeast Saccharomyces cerevisiae. *J. Gen. Microbiol.* **137**, 341–349 (1991).
10. Thevelein, J. M. Fermentable sugars and intracellular acidification as specific activators of the RAS-adenylate cyclase signalling pathway in yeast: the relationship to nutrient-induced cell cycle control. *Mol. Microbiol.* **5**, 1301–1307 (1991).
11. Mbonyi, K., Beullens, M., Detremerie, K., Geerts, L. & Thevelein, J. M. Requirement of one functional RAS gene and inability of an oncogenic ras variant to mediate the glucose-induced cyclic AMP signal in the yeast Saccharomyces cerevisiae. *Mol. Cell. Biol.* **8**, 3051–3057 (1988).
12. Kataoka, T., Broek, D. & Wigler, M. DNA sequence and characterization of the S. cerevisiae gene encoding adenylate cyclase. *Cell* **43**, 493–505 (1985).
13. Casperson, G. F., Walker, N. & Bourne, H. R. Isolation of the gene encoding adenylate cyclase in Saccharomyces cerevisiae. *Proc. Natl. Acad. Sci. U. S. A.* **82**, 5060–3 (1985).
14. Thevelein, J. M. *et al.* Regulation of the cAMP level in the yeast Saccharomyces cerevisiae: intracellular pH and the effect of membrane depolarizing compounds. *J. Gen. Microbiol.* **133**, 2191–2196 (1987).
15. Rolland, F. *et al.* The role of hexose transport and phosphorylation in cAMP signalling in the yeast Saccharomyces cerevisiae. *FEMS Yeast Res.* **1**, 33–45 (2001).
16. Kim, J., Roy, A. & Ii, D. J. Biochimica et Biophysica Acta The glucose signaling network in yeast. *BBA - Gen. Subj.* **1830**, 5204–5210 (2013).
17. Yun, C., Tamaki, H., Nakayama, R., Yamamoto, K. & Kumagai, H. Gpr1p, a Putative G-Protein Coupled Receptor, Regulates Glucose-Dependent Cellular cAMP Level in Yeast Saccharomyces cerevisiae. *Biochem. Biophys. Res. Commun.* **252**, 29–33 (1998).
18. van Aelst, L., Boy-marcotte, E., Camonis, J. H., Thevelein, J. M. & Jacquet, M. The C-terminal part of the CDC25 gene product plays a key role in signal transduction in the glucose-induced modulation of CAMP level in Saccharomyces cerevisiae. *Eur. J. Biochem.* **6680**, 675–680 (1990).
19. Broek, D. *et al.* The S . cerevisiae CDC25 Gene Product Regulates the RAS/Adenylate Cyclase Pathway. *Cell* **48**, 789–799 (1987).
20. Munder, T. & Küntzel, H. Glucose-induced CAMP signaling in Saccharomyces cerevisiae is mediated by the CDC25 protein. *Fed. Eur. Biochem. Soc.* **242**, 341–345 (1989).
21. Kraakman, L. *et al.* A Saccharomyces cerevisiae G-protein coupled receptor, Gpr1, is specifically required for glucose activation of the cAMP pathway during the transition to growth on glucose. *Mol. Microbiol.* **32**, 1002–1012 (1999).
22. Lemaire, K., Van De Velde, S., Van Dijck, P. & Thevelein, J. M. Glucose and sucrose act as agonist and mannose as antagonist ligands of the G protein-coupled receptor Gpr1 in the yeast Saccharomyces cerevisiae. *Mol. Cell* **16**, 293–299 (2004).
23. Rolland, F. *et al.* Glucose-induced cAMP signalling in yeast requires both a G-protein coupled receptor system for extracellular glucose detection and a separable hexose kinase-dependent sensing process. *Mol. Microbiol.* **38**, 348–358 (2000).
24. Johnson, K. E., Cameron, S., Wiglers, M. & Zollers, M. J. Expression in Escherichia coli of B C Y l , the Regulatory Subunit of Cyclic AMP-dependent Protein Kinase from Saccharomyces cereuisiae. *J. Biol. Chem.* **262**, 8636–8642 (1987).
25. Toda, T. *et al.* Cloning and characterization of BCY1, a locus encoding a regulatory subunit of the cyclic AMP-dependent protein kinase in Saccharomyces cerevisiae. *Mol. Cell. Biol.* **7**, 1371–7 (1987).
26. Hixsons, C. S. & Krebs, E. G. Characterization of a Cyclic AMP-binding Protein from Bakers ' Yeast. *J. Biol. Chem.* **255**, 2137–2145 (1980).
27. Martinez-Pastor1, M. T. *et al.* The Saccharomyces cerevisiae zinc finger proteins Msn2p and Msn4p are required for

transcriptional induction through the stress-response element (STRE). *EMBO J.* **15**, 2227–2235 (1996).
28. Vidan, S. & Mitchell, a P. Stimulation of yeast meiotic gene expression by the glucose-repressible protein kinase Rim15p. *Mol. Cell. Biol.* **17**, 2688–2697 (1997).
29. Reinders, A., Bürckert, N., Boller, T., Wiemken, A. & De Virgilio, C. Saccharomyces cerevisiae cAMP-dependent protein kinase controls entry into stationary phase through the Rim15p protein kinase. *Genes Dev.* **12**, 2943–55 (1998).
30. Smith, A., Ward, M. P. & Garrett, S. Yeast PKA represses Msn2p/Msn4p-dependent gene expression to regulate growth, stress response and glycogen accumulation. *EMBO J.* **17**, 3556–3564 (1998).
31. van der Plaat, J. B. Cyclic 3′,5′-adenosine monophosphate stimulates trehalose degradation in baker's yeast. *Biochem. Biophys. Res. Commun.* **56**, 580–587 (1974).
32. Hardy, T. A., Huang, D. & Roach, P. J. Interactions between cAMP-dependent and SNF1 protein kinases in the control of glycogen accumulation in Saccharomyces cerevisiae. *J. Biol. Chem.* **269**, 27907–13 (1994).
33. Winderickx, J. *et al.* Regulation of genes encoding subunits of the trehalose synthase complex in Saccharomyces cerevisiae: Novel variations of STRE-mediated transcription control? *Mol. Gen. Genet.* **252**, 470–482 (1996).
34. Pohlig, G. & Holzer, H. Phosphorylation and Inactivation of Yeast Fructose-1,6- bisphosphatase by Cyclic AMP-dependent Protein Kinase from Yeast. *J. Biol. Chem.* **260**, 13818–13823 (1985).
35. Hofmann, E., Bedri, A., Kessler, R., Kretschmer, M. & Schellenberger, W. 6-Phosphofructo-2-kinase and fructose-2,6-bisphosphatase from Saccharomyces cerevisiae. *Adv. Enzyme Regul.* **28**, 283–306 (1989).
36. Dihazi, H., Kessler, R. & Eschrich, K. Glucose-Induced Stimulation of the Ras-cAMP Pathway in Yeast Leads to Multiple Phosphorylations and Activation of 6-Phosphofructo-2-kinase. 6275–6282 (2003).
37. Park, J. I., Grant, C. M. & Dawes, I. W. The high-affinity cAMP phosphodiesterase of Saccharomyces cerevisiae is the major determinant of cAMP levels in stationary phase: Involvement of different branches of the Ras-cyclic AMP pathway in stress responses. *Biochem. Biophys. Res. Commun.* **327**, 311–319 (2005).
38. Nikawa, J., Sass, P. & Wigler, M. Cloning and characterization of the low-affinity cyclic AMP phosphodiesterase gene of Saccharomyces cerevisiae. *Mol. Cell. Biol.* **7**, 3629–36 (1987).
39. Ma, P., Wera, S., Van Dijck, P. & Thevelein, J. M. The PDE1-encoded Low-Affinity Phosphodiesterase in the Yeast Saccharomyces cerevisiae Has a Specific Function in Controlling Agonist-induced cAMP Signaling. *Mol. Biol. Cell* **10**, 91–104 (1999).
40. Tanaka, K., Matsumoto, K. & Toh-E, A. IRA1, an inhibitory regulator of the RAS-cyclic AMP pathway in Saccharomyces cerevisiae. *Mol. Cell. Biol.* **9**, 757–68 (1989).
41. Tanaka, K. *et al.* IRA2, a second gene of Saccharomyces cerevisiae that encodes a protein with a domain homologous to mammalian ras GTPase-activating protein. *Mol. Cell. Biol.* **10**, 4303–4313 (1990).
42. Versele, M., de Winde, J. H. & Thevelein, J. M. A novel regulator of G protein signalling in yeast, Rgs2, downregulates glucose-activation of the cAMP pathway through direct inhibition of Gpa2. *EMBO J.* **18**, 5577–91 (1999).
43. Dong, J. & Bai, X. The membrane localization of Ras2p and the association between Cdc25p and Ras2-GTP are regulated by protein kinase A (PKA) in the yeast Saccharomyces cerevisiae. *FEBS Lett.* **585**, 1127–34 (2011).
44. Stewart-Ornstein, J., Chen, S., Bhatnagar, R., Weissman, J. S. & El-Samad, H. Model-guided optogenetic study of PKA signaling in budding yeast. *Mol. Biol. Cell* **28**, 221–227 (2017).
45. Peeters, K. *et al.* Fructose-1,6-bisphosphate couples glycolytic flux to activation of Ras. *Nat. Commun.* **8**, (2017).
46. Ma, P., Goncalves, T., Maretzek, A., Dias, M. C. L. & Thevelein, J. M. The lag phase rather than the exponential-growth phase on glucose is associated with a higher cAMP level in wild-type and cAPK-attenuated strains of the yeast Saccharomyces cerevisiae. *Microbiology* **143**, 3451–3459 (1997).
47. Thevelein, J. M. & de Winde, J. H. Novel sensing mechanisms and targets for the cAMP-protein kinase A pathway in the yeast Saccharomyces cerevisiae. *Mol. Microbiol.* **33**, 904–918 (1999).
48. Eraso, P. & Gancedo, J. M. Catabolite repression in yeasts is not associated with low levels of cAMP. *Eur. J. Biochem.* **141**, 195–198 (1984).
49. Delvigne, F., Zune, Q., Lara, A. R., Al-Soud, W. & Sørensen, S. J. Metabolic variability in bioprocessing: Implications of microbial phenotypic heterogeneity. *Trends Biotechnol.* **32**, 608–616 (2014).
50. Altschuler, S. J. & Wu, L. F. Cellular Heterogeneity: Do Differences Make a Difference? *Cell* **141**, 559–563 (2010).
51. Xiao, Y., Bowen, C. H., Liu, D. & Zhang, F. Exploiting nongenetic cell-to-cell variation for enhanced biosynthesis. *Nat. Chem. Biol.* **12**, 339–344 (2016).
52. Takhaveev, V. & Heinemann, M. Metabolic heterogeneity in clonal microbial populations. *Curr. Opin. Microbiol.* **45**, 30–38 (2018).
53. van der Krogt, G. N. M., Ogink, J., Ponsioen, B. & Jalink, K. A Comparison of Donor-Acceptor Pairs for Genetically Encoded FRET Sensors: Application to the Epac cAMP Sensor as an Example. *PLoS One* **3**, e1916 (2008).
54. Ponsioen, B. *et al.* Detecting cAMP-induced Epac activation by fluorescence resonance energy transfer: Epac as a novel cAMP indicator. *EMBO Rep.* **5**, 1176–1180 (2004).
55. Botman, D., de Groot, D. H., Schmidt, P., Goedhart, J. & Teusink, B. In vivo characterisation of fluorescent proteins in budding yeast. *Sci. Rep.* **9**, 2234 (2019).
56. Mastop, M. *et al.* Characterization of a spectrally diverse set of fluorescent proteins as FRET acceptors for mTurquoise2. *Sci. Rep.* **7**, 11999 (2017).
57. Gietz, R. D. & Schiestl, R. H. Quick and easy yeast transformation using the LiAc/SS carrier DNA/PEG method. *Nat. Protoc.* **2**, 35–37 (2007).

58. Hansen, A. S., Hao, N. & O'Shea, E. K. High-throughput microfluidics to control and measure signaling dynamics in single yeast cells. *Nat. Protoc.* **10**, 1181–97 (2015).
59. Klarenbeek, J., Goedhart, J., Van Batenburg, A., Groenewald, D. & Jalink, K. Fourth-generation Epac-based FRET sensors for cAMP feature exceptional brightness, photostability and dynamic range: Characterization of dedicated sensors for FLIM, for ratiometry and with high affinity. *PLoS One* **10**, 1–11 (2015).
60. Cranfill, P. J. *et al.* Quantitative assessment of fluorescent proteins. *Nat. Methods* **13**, 557–562 (2016).
61. Russell, M., Bradshaw-Rouse, J., Markwardt, D. & Heideman, W. Changes in gene expression in the Ras/adenylate cyclase system of Saccharomyces cerevisiae: correlation with cAMP levels and growth arrest. *Mol Biol Cell* **4**, 757–765 (1993).
62. Xu, Z. & Tsurugi, K. A potential mechanism of energy-metabolism oscillation in an aerobic chemostat culture of the yeast Saccharomyces cerevisiae. *FEBS J.* **273**, 1696–1709 (2006).
63. Magherini, F. *et al.* In Saccharomyces cerevisiae an unbalanced level of tyrosine phosphorylation down-regulates the Ras/PKA pathway. *Int. J. Biochem. Cell Biol.* **38**, 444–460 (2006).
64. Vanhalewyn, M. *et al.* A mutation in Saccharomyces cerevisiae adenylate cyclase, Cyr1(K1876M), specifically affects glucose- and acidification-induced cAMP signalling and not the basal cAMP level. *Mol. Microbiol.* **33**, 363–376 (1999).
65. Ferrell, J. E. Signaling Motifs and Weber's Law. *Mol. Cell* **36**, 724–727 (2009).
66. Adler, M. & Alon, U. Fold-change detection in biological systems. *Curr. Opin. Syst. Biol.* **8**, 81–89 (2018).
67. Canelas, A. B., Ras, C., ten Pierick, A., van Gulik, W. M. & Heijnen, J. J. An in vivo data-driven framework for classification and quantification of enzyme kinetics and determination of apparent thermodynamic data. *Metab. Eng.* **13**, 294–306 (2011).
68. Van Hoek, P., Van Dijken, J. P. & Pronk, J. T. Effect of specific growth rate on fermentative capacity of baker's yeast. *Appl. Environ. Microbiol.* **64**, 4226–4233 (1998).
69. Colombo, S. *et al.* Detection of cAMP and of PKA activity in Saccharomyces cerevisiae single cells using Fluorescence Resonance Energy Transfer (FRET) probes. *Biochem. Biophys. Res. Commun.* **487**, 594–599 (2017).
70. Bermejo, C., Haerizadeh, F., Sadoine, M. S. C., Chermak, D. & Frommer, W. B. Differential regulation of glucose transport activity in yeast by specific cAMP signatures. *Biochem. J.* **452**, 489–497 (2013).
71. Besozzi, D. *et al.* The role of feedback control mechanisms on the establishment of oscillatory regimes in the Ras/cAMP/PKA pathway in S. cerevisiae. *EURASIP J. Bioinforma. Syst. Biol.* **2012**, 10 (2012).
72. van Heerden, J. H. *et al.* Lost in transition: start-up of glycolysis yields subpopulations of nongrowing cells. *Science* **343**, 1245114 (2014).
73. Botman, D. & Teusink, B. *Dynamic ATP measurements in budding yeast reveal single-cell heterogeneity. In preparation.* (2019).
74. Youk, H. & van Oudenaarden, A. Growth landscape formed by perception and import of glucose in yeast. *Nature* **462**, 875–879 (2009).
75. Lee, R. E. C., Walker, S. R., Savery, K., Frank, D. A. & Gaudet, S. Fold change of nuclear NF-κB determines TNF-induced transcription in single cells. *Mol. Cell* **53**, 867–879 (2014).
76. Kamino, K. *et al.* Fold-change detection and scale invariance of cell–cell signaling in social amoeba. *Proc. Natl. Acad. Sci.* **114**, E4149–E4157 (2017).
77. Frick, C. L., Yarka, C., Nunns, H. & Goentoro, L. Sensing relative signal in the Tgf-β/Smad pathway. *Proc. Natl. Acad. Sci.* **114**, E2975–E2982 (2017).
78. Ruan, Y.-L. Sucrose metabolism: gateway to diverse carbon use and sugar signaling. *Annu. Rev. Plant Biol.* **65**, 33–67 (2014).
79. Van de Velde, S. & Thevelein, J. M. Cyclic AMP-Protein Kinase A and Snf1 Signaling Mechanisms Underlie the Superior Potency of Sucrose for Induction of Filamentation in Saccharomyces cerevisiae. *Eukaryot. Cell* **7**, 286–293 (2008).
80. Reijenga, K. A. *et al.* Control of Glycolytic Dynamics by Hexose Transport in Saccharomyces cerevisiae. *Biophys. J.* **80**, 626–634 (2001).
81. Reifenberger, E., Boles, E. & Ciriacy, M. Kinetic characterization of individual hexose transporters of Saccharomyces cerevisiae and their relation to the triggering mechanisms of glucose repression. *Eur. J. Biochem.* **245**, 324–33 (1997).
82. Lohr, D., Venkov, P. & Zlatanova, J. Transcriptional regulation in the yeast GAL gene family: a complex genetic network. *FASEB J.* **9**, 777–787 (1995).
83. Ozcan, S. & Johnston, M. Three different regulatory mechanisms enable yeast hexose transporter (HXT) genes to be induced by different levels of glucose. *Mol. Cell. Biol.* **15**, 1564–1572 (1995).
84. Paulo, J. A. *et al.* Quantitative mass spectrometry-based multiplexing compares the abundance of 5000 S. cerevisiae proteins across 10 carbon sources. *J. Proteomics* **148**, 85–93 (2016).
85. Paulo, J. A., O'Connell, J. D., Gaun, A. & Gygi, S. P. Proteome-wide quantitative multiplexed profiling of protein expression: Carbon-source dependency in Saccharomyces cerevisiae. *Mol. Biol. Cell* **26**, 4063–4074 (2015).
86. Eraso, P., Mazón, M. J. & Gancedo, J. M. Internal acidification and cAMP increase are not correlated in Saccharomyces cerevisiae. *Eur. J. Biochem.* **165**, 671–4 (1987).

Supplements

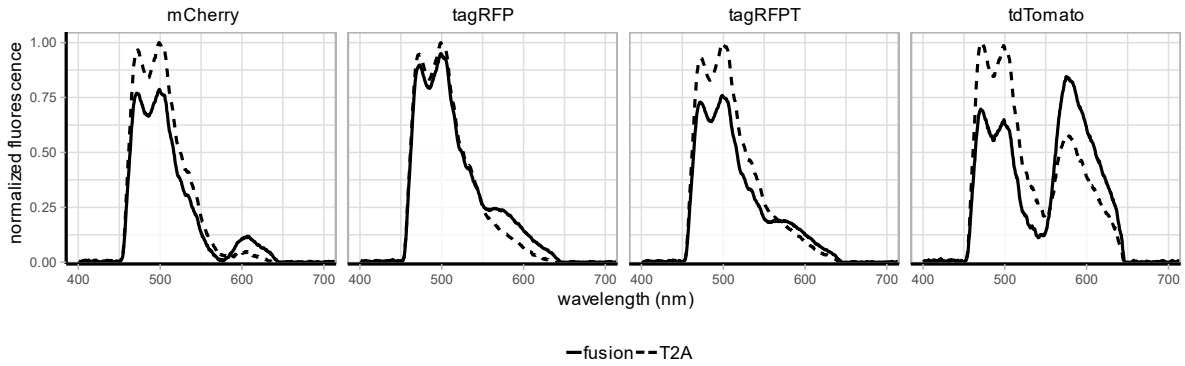

Figure S1. Spectral analysis of potential acceptors for mTq2. Solid lines show direct fusions of the depicted FP with mTq2. Dotted lines show spectra of the T2A fusion with mTq2, resulting in equimolar expression of cleaved mTq2 and acceptor, used as non-FRET control. Spectra of plated W303-1A colonies were recorded.

Table S1. FRET efficiencies determined by frequency domain lifetime measurements of W303-1A colonies expressing the fusion constructs or mTq2. [a]calculated lifetime of mTq2 determined by frequency domain. [b]FRET efficiency calculated as (1-($Lifetime_{donor+acceptor}$/$lifetime_{donor}$))*100.

Fusion	Lifetime[a]	FRET efficiency[b]
mCherry-mTq2	3.29 ns	12.5
tagRFP-mTq2	3.73 ns	0.8
tagRFPT-mTq2	3.47 ns	7.7
TdTomato-mTq2	2.9 ns	22.9
mTq2	3.76 ns	n/a

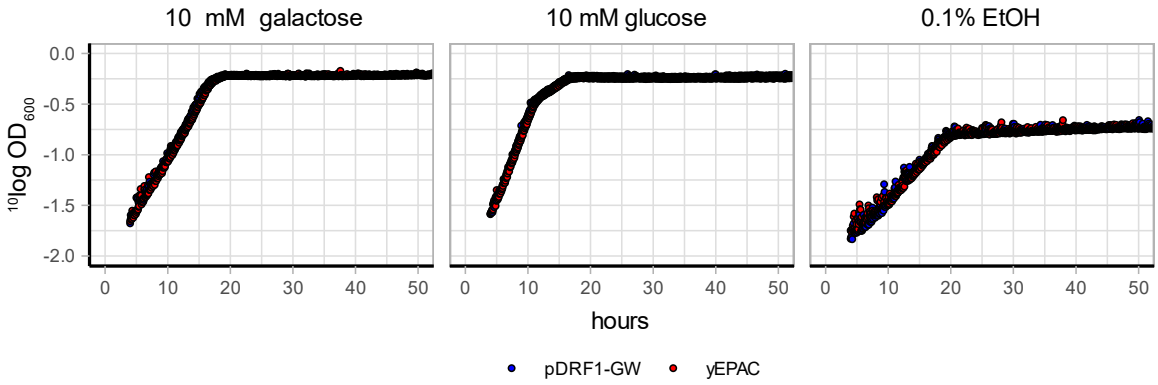

Figure S2. Growth curves of W303-1A WT cells expressing either yEPAC or the empty pDRF1-GW vector. Cells were grown to midlog in 1x YNB containing 1% EtOH, washed and resuspended in medium containing either 10 mM galactose, 10 mM glucose or 0.1% EtOH. Points indicate mean OD, color indicates the strain.

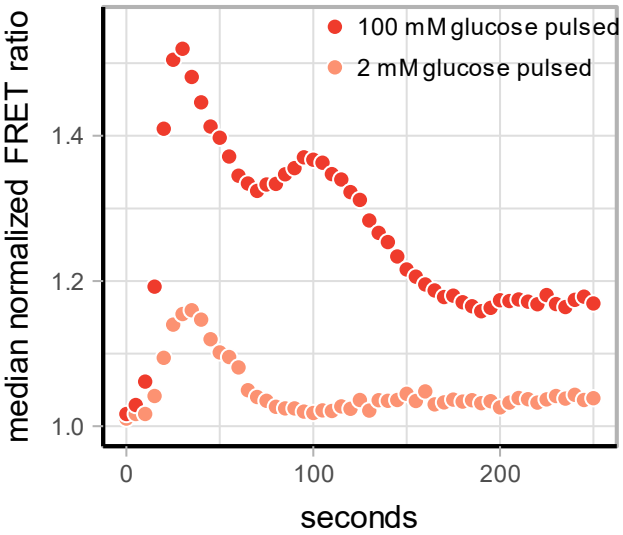

Figure S3. Dynamic flow-cytometry FRET measurements. B) W303-1A WT cells were grown on 1% EtOH, a baseline was recorded (not shown in graph) and a glucose pulse was added. The first obtained timepoint after glucose addition is set to t=0 seconds. Median FRET ratio for every binned timepoint are shown, depicted by the points. Point color indicate amount of glucose pulsed.

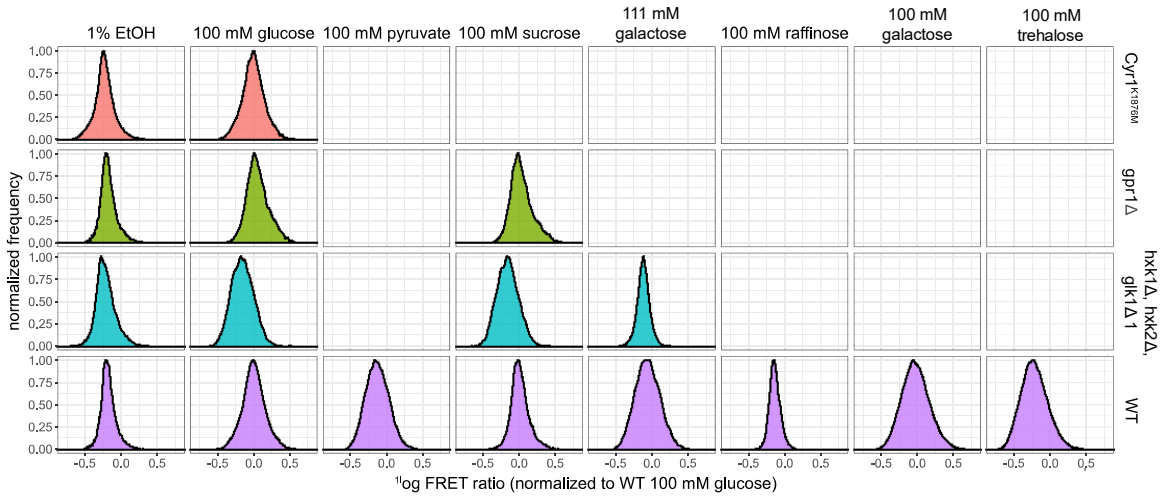

Figure S4. Flow cytometry distributions. A) Normalized frequency results of flow-cytometry readouts (all biological replicates combined), normalized to W303-1A WT cells growing on glucose. Substrate used is shown above each column, various strains are depicted at the right side.

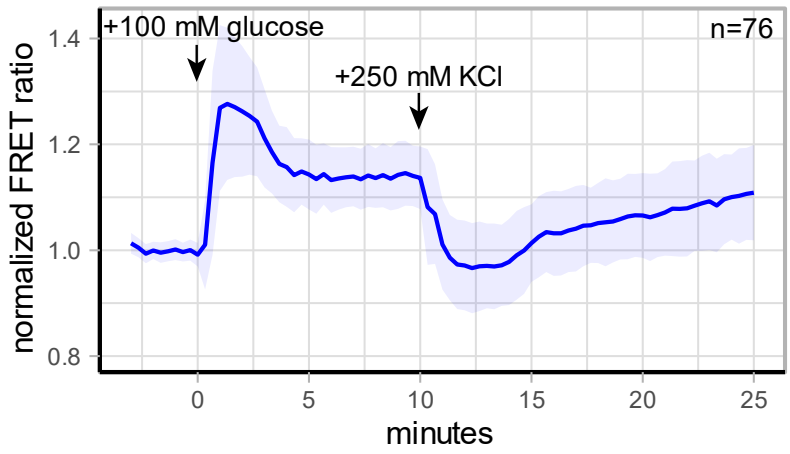

Figure S5. yEPAC FRET responses during salt stress. W303-1A WT cells grown on 1% ethanol were pulsed with 100 mM glucose at 0 minutes and with 250 mM KCl at 10 minutes (indicated with arrows). Lines show mean FRET ratios (corrected for the yEPAC-R279L response), normalized to the baseline, shaded areas indicate SD.

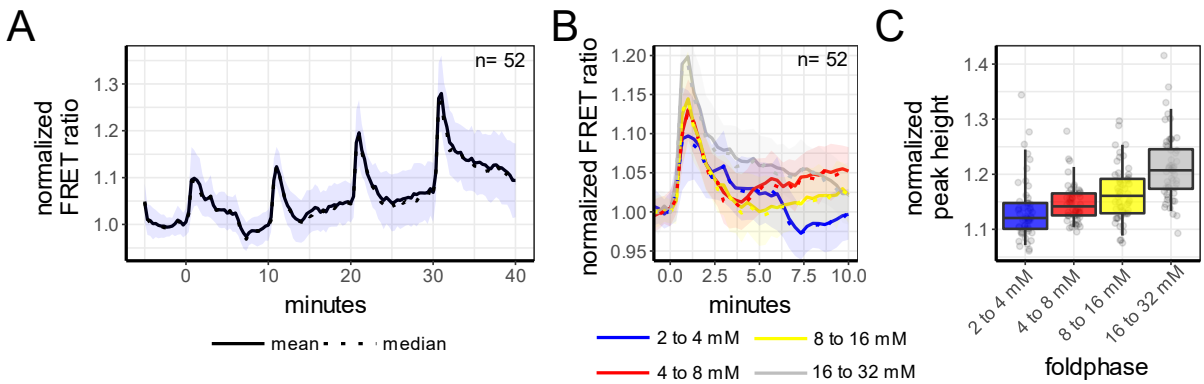

Figure S6. Weber's law of the same cells in time, with 10 minutes periods in between. A) W303-1A cells expressing yEPAC were pre-incubated on 2 mM glucose. Afterwards, cells were transitioned to 4 mM glucose at t=0 minutes and transitioned again to 8 mM at t=25 minutes. Lines show population mean response, normalized to the first 5 minutes, shaded areas indicate SD. B) Responses of the transitions performed in graph A, normalized to the last 3 frames before each transition. Colour indicates the transition. C) Boxplot of the peak heights of each cells for each transition. Dots show single-cell peak heights, boxes indicate median with quartiles, whiskers indicate the 0.05–0.95 fraction of the datapoints. D) Relation of normalized peak heights of single-cells between the first and second transitions. Dots represents single-cells.

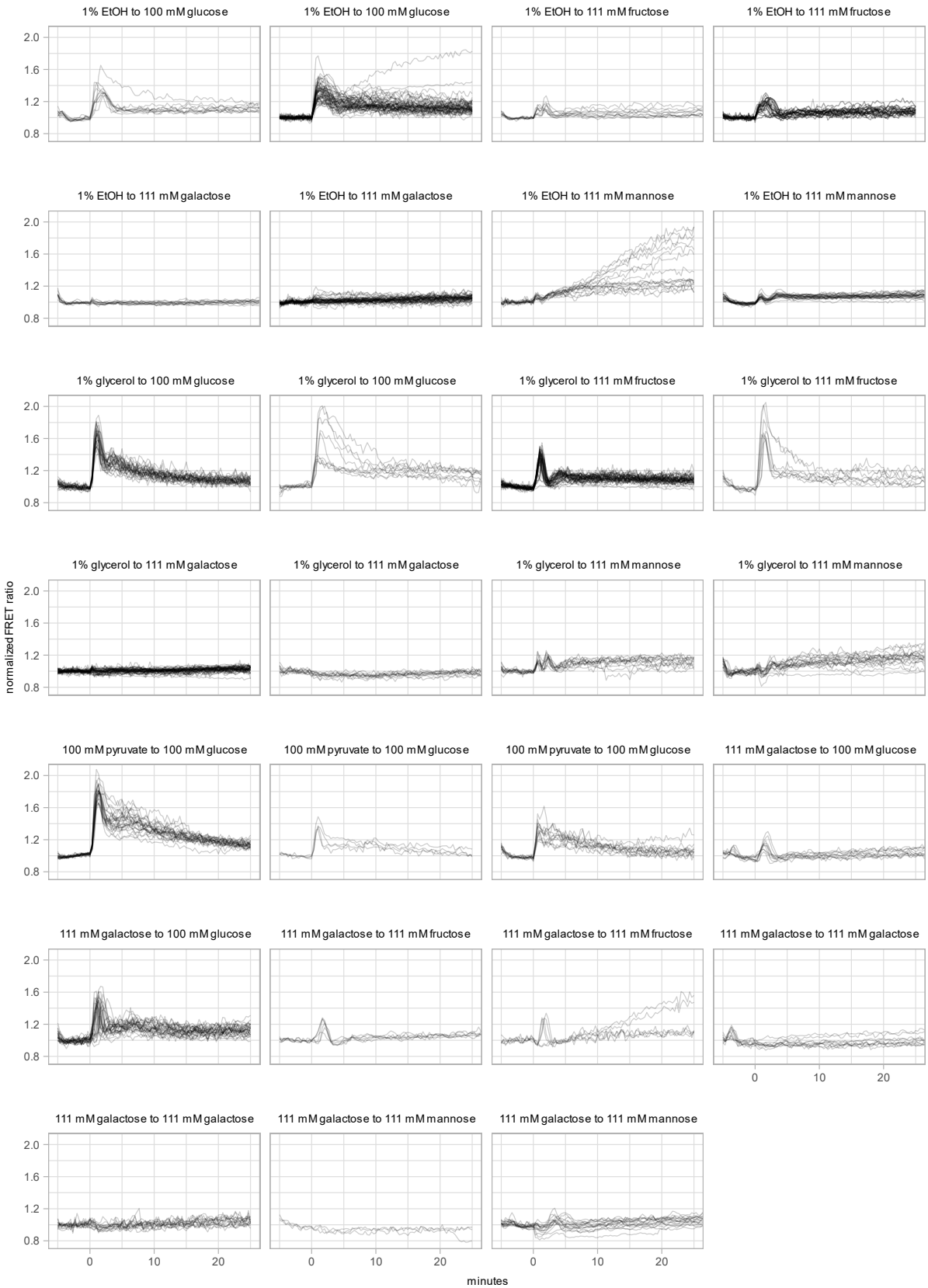

Figure S7. Single-cell yEPAC FRET responses of various carbon transitions. Cells growing on various non-fermentative carbon sources were pulsed with various sugars (transitions depicted above each panel) at 0 minutes. Lines show baseline-normalized FRET ratios of each cell.

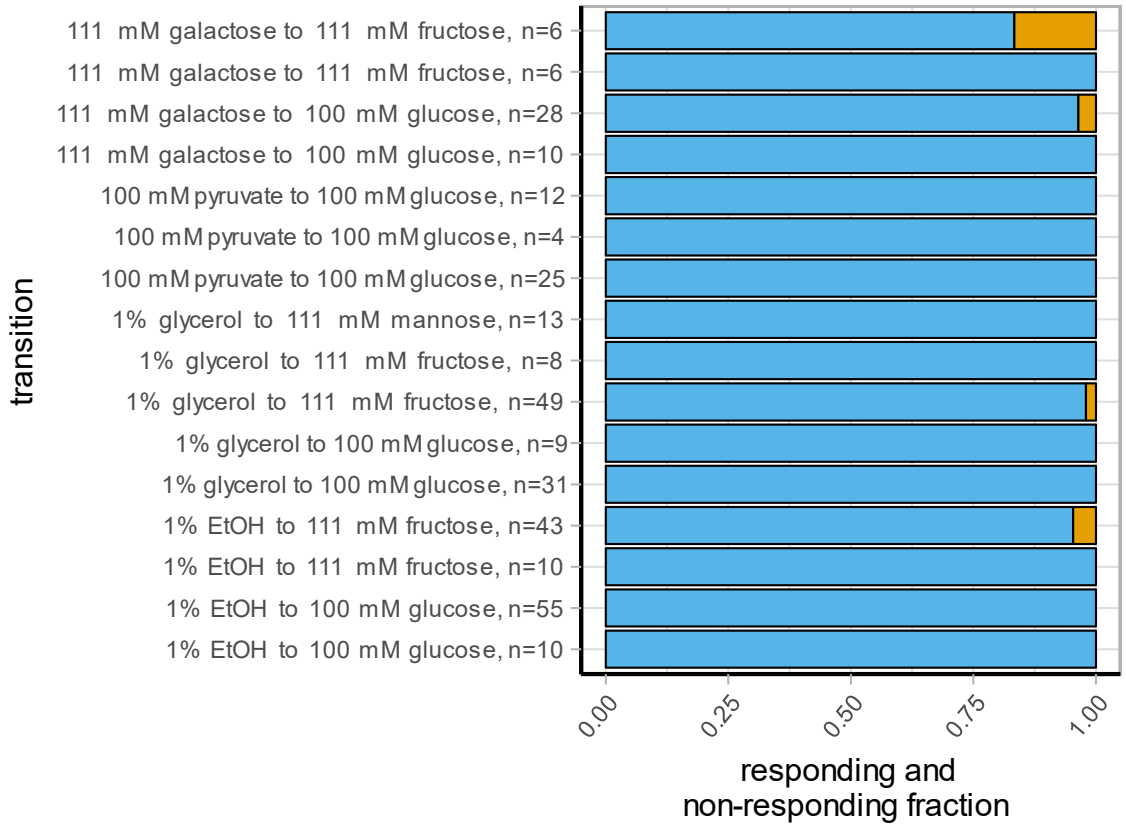

Figure S8. Fraction of responding (blue bars) and non-responding (orange bars) for the various glucose and fructose transitions. Only transitions that showed a population-average peak height of at least 1.15 were used. Cells were considered as responding when they showed a peak height of at least 30% of the mean peak value for the specific transition.